





### 3.2. Wavelet Thresholding

Most of the wavelet denoising techniques are based on the wavelet coefficient shrinkage procedure for discrete wavelet transform [13]. The two more popular thresholding schemes are the so-called soft and hard-thresholding. In both cases, the threshold level is proportional to the noise standard deviation. Hard thresholding consists in putting to zero wavelet coefficients of amplitude smaller than threshold. Soft-thresholding additionally reduces the amplitude of the other coefficients by the threshold quantity. The soft thresholding rule is normally chosen, because it has been shown to achieve near-optimal minimax rate, and the optimal soft thresholding estimator yields a smaller risk than the optimal hard thresholding estimator.

Let  $W$  and  $W^{-1}$  denote the two dimensional orthogonal discrete wavelet transform (DWT) matrix and its inverse respectively. Then  $y = Ws$  represents the matrix of wavelet coefficients of  $s$  having four subbands ( $LL$ ,  $LH$ ,  $HL$  and  $HH$ ) [14, 15]. The subbands  $HH_j$ ,  $HL_j$ ,  $LH_j$  are called details, where  $j$  is the scale varying from 1 to  $J$  and  $J$  is the total number of decompositions. The subband  $LL_j$  is the low-resolution residue. The wavelet thresholding denoising method processes each coefficient of  $y$  from the detail subbands with a soft threshold function to obtain  $y^*$ . The denoised estimate is inverse transformed to  $s^* = W^{-1}y^*$ . The procedure removes noise by thresholding only the wavelet coefficients of the detail subbands, while keeping the low-resolution coefficients unaltered. We describe here the method for computing the threshold value  $T_n$ , which is adaptive to different subband characteristics [16]

$$T_n = \beta \frac{\sigma^2}{\sigma_y}$$

Where, the scale parameter  $\beta$  is computed once for each scale using the following equation

$$\beta = \sqrt{\log(L_k / J)}$$

$L_k$  is the length of the subband at  $k^{\text{th}}$  scale and  $J$  is the total number of decompositions.  $\sigma_y$  is the standard deviation of the subband under consideration.  $\sigma$  is the noise variance, which is estimated from the subband  $HH_1$ , using the formula [14,17]

$$\sigma^2 = \left[ \frac{\text{median}(|y_{ij}|)}{0.6745} \right]^2 \quad y_{ij} \in \text{subband}HH_1$$

### 4. Numerical Results

A number of computer simulations were carried out in which synthetic digital holograms were generated. The investigated volume (Fig.2) is represented by three planes  $P_1$ ,  $P_2$  and  $P_3$  which contain tracer particles randomly distributed. The planes ( $P_1$ ,  $P_2$  and  $P_3$ ) separation distance is  $\Delta z = 250 \mu\text{m}$ . The wavelength of illuminating light is  $\lambda = 0.63 \mu\text{m}$ . The particle size is in the range of  $20 \mu\text{m}$ . The number of particles is about 80 by plane. The recording hologram distance (between object plane and hologram plane) is  $z = 50 \text{ mm}$ . The two holograms  $I_z$  and  $I_{2z}$  generated by simulation are shown in Fig.3. The size of the holograms is a  $256 \times 256$  pixel.

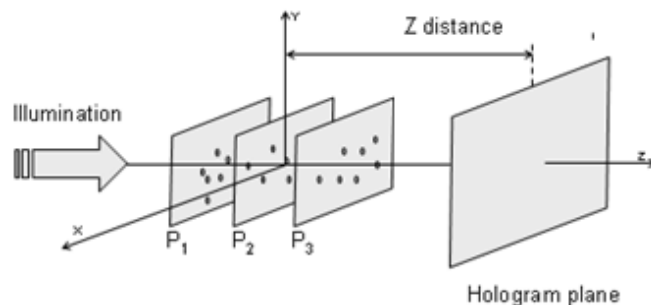
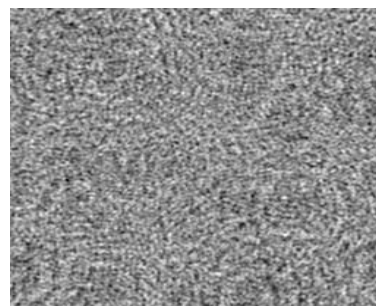
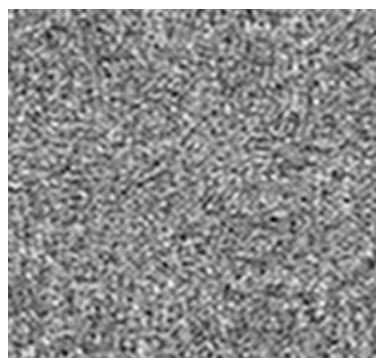


Figure 2: Synthetic volume seeded with tracer particle

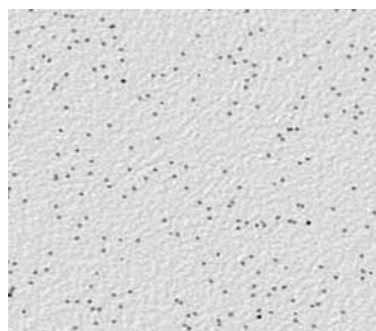


(a)

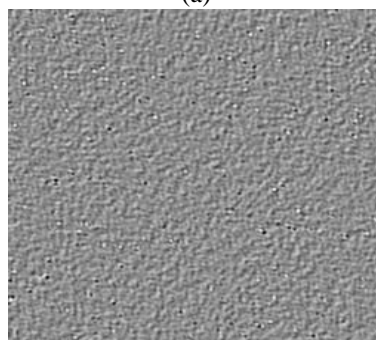


(b)

Figure 3: (a) The hologram  $I_z$  and (b) the hologram  $I_{2z}$



(a)



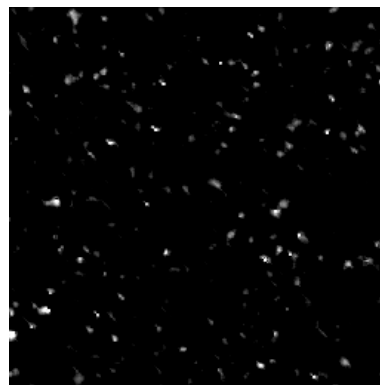
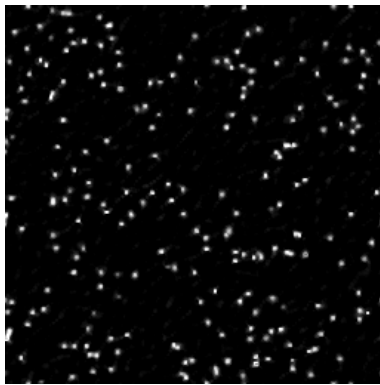
(b)

Figure 4: The reconstructed object ( $P_2$  plane): (a) the absorption and (b) the phase shift

In Fig.4 we present the absorption  $a(x, y)$  and phase shift  $\phi(x, y)$  of plane  $P_2$  obtained by the two in-line holograms reconstruction algorithm.

The wavelet transform employs Daubachies wavelet with four vanishing moments at four scales of decomposition. After the DWT decomposition, the absorption and phase shift images are denoized by shrinkage the coefficients from the detail Subbands with a Soft-thresholding. The procedure removes noise by thresholding only the wavelet coefficients of the detail subbands HL, LH and HH, while keeping the low- resolution coefficients LL unaltered. The threshold value is adaptive to different subband characteristics. The denoised absorption and phase shift images are shown Fig.5. The wavelet thresholding method, give a good result.

The velocity vector field of each plane is computed by applying PIV (Particle Image Velocimetry) algorithm [18]. The determined velocity vector field of the reconstructed plane  $P_2$  is show Fig.7. The PSNR is equal to 28.65 dB.



**Figure 5:** (a) the denoised absorption image and (b) the denoised phase shift image



**Figure 6:** The reconstructed plane ( $P_2$ ): particle image

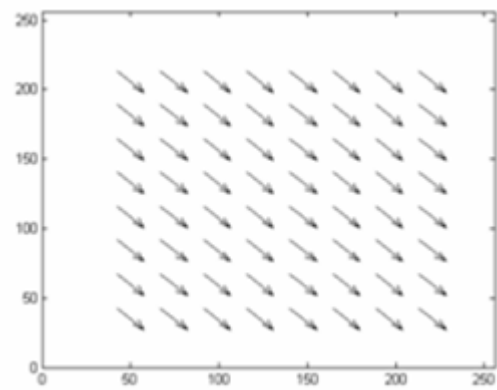


**Figure 7:** The plane ( $P_2$ ) velocity field

## 5. Conclusion

Digital Holographic Particle Image Velocimetry is a promising technique for flow field measurement. However, the low resolution of the sensors still remains poor and needs to be compensated by image processing techniques. In this article, we had presented the two in-line holograms algorithm. This algorithm permits, at the same time, to retrieve the absorption, the phase shift images. The use of the phase shift information to particle localization permits to increase the accuracy along the depth direction. A wavelet thresholding method is employed to remove noise in the reconstructed absorption and phase shift by using a simple subband adaptive threshold. In the computer simulation, we had demonstrated that this method can be applied to flow field measurement. The obtained results are good.

## References

- [1] J. W. Goodman, R.W. Lawrence. "Digital image formation from electronically detected holograms" *Appl Phys Let*; **11**, 77-79 (1967)
- [2] L. P. Yaroslavskii, N. S. Merzlyakov. "Methods of digital holography". *Consultants Bureau, New York* (1980)
- [3] M. Adams, T. Kreis, W. Juptner. "Particle size and position measurement with digital holography". *Proc SPIE*; **3098**, 234-240 (1997)
- [4] T. Xiao, H. Xu, Y. Zhang, J. Chen, and Z. Xu. "Digital image decoding for in-line X-ray holography using two holograms". *J Mod Opt*; **45**, 343-353 (1998)
- [5] S. G. Mallat. "Wavelet tour of signal processing", 2<sup>nd</sup> edition, (*Academic Press, 1999*)
- [6] D.L. Donoho."De-Noising by Soft Thresholding", *IEEE Trans Info Theory* 43, pp. 933-936, 1993
- [7] S. G. Chang, B. Yu and M. Vattereli. "Adaptive Wavelet Thresholding for Image Denoising and Compression", *IEEE Trans Image Processing*; vol. 9, pp. 1532-1546, Sept. 2000.
- [8] M. Jansen. "Noise Reduction by Wavelet Thresholding". *Springer Verlag New York Inc.- 2001*.
- [9] L. Onural, P. D. Scott. "Digital decoding of in-line holograms". *Opt. Eng.* **26**, 1124-1132 (1987)
- [10] L. Onural. "Diffraction from a wavelet point of view". *Opt Lett*; **18**, 846-848 (1993)

- [11] Y. Meyer. "Wavelets: algorithms & applications", *Society for industrial and Applied Mathematics*, Philadelphia, (1993).
- [12] I. Daubachies. "Ten lectures on wavelets", *Society for industrial and Applied Mathematics*, Philadelphia, (1992).
- [13] D.L. Donoho. "Denoising by soft thresholding". *IEEE Transactions on information theory*; 41,613-627, 1995
- [14] M. Vattereli and J. Kovacevic. "Wavelets and Subband Coding", *Englewood Cliffs, NJ, Prentice Hall*, 1995.
- [15] Savita Gupta and Lakhwinder kaur. "Wavelet Based Image Compression using Daubechies Filters", *In proc 8th National conference on communications*; I.I.T. Bombay, NCC-2002.
- [16] L. Kaur, S. Gupta, R.C. Chauhan. "Image denoising using Wavelet Thresholding", [Online] Available: <http://www.ee.iitb.ac.in/~icvgip/PAPERS/202.pdf>
- [17] P.H. Westrink, J. Biemond and D.E. Boekee. "An optimal bit allocation algorithm for subband coding", *in Proc IEEE Int; Conf Acoustics Speech Signal Processing*, Dallas, TX, April 1987, pp. 1378-1381.
- [18] C.E. Willert, M. Gharib. "Digital particle image Velocimetry", *Exp. Fluids* **10**, 181-193 (1999)